THE JOURNAL OF PHYSICAL CHEMISTRY LETTERS
A JOURNAL OF THE AMERICAN CHEMICAL SOCIETY

pubs.acs.org/JPCL Letter

Size-Specific Infrared Spectroscopic Study of the Reactions between Water Molecules and Neutral Vanadium Dimer: Evidence for Water Splitting

Huijun Zheng, Shuai Jiang, Wenhui Yan, Tiantong Wang, Shangdong Li, Hua Xie, Gang Li,* Xueming Yang, and Ling Jiang*

Cite This: J. Phys. Chem. Lett. 2023, 14, 3878−3883 Read Online

ACCESS | Metrics & More | Article Recommendations | Supporting Information

ABSTRACT: Investigation of the reactions between water molecules and neutral metal clusters is important in water splitting but is very challenging due to the inherent difficulty of size selection. Here, we report a size-specific infrared-vacuum ultraviolet spectroscopic study on the reactions of water with neutral vanadium dimer. The $V_2O_3H_4$ and $V_2O_4H_6$ products were characterized to have unexpected $V_2(\mu_2\text{-OH})(\mu_2\text{-H})(\eta^1\text{-OH})_2$ and $V_2(\mu_2\text{-OH})_2(\eta^1\text{-H})_2(\eta^1\text{-OH})_2$ structures, indicative of a water decomposition. A combination of theory and experiment reveals that the water splitting by V_2 is both thermodynamically exothermic and kinetically facile in the gas phase. The present system serves as a model for clarifying the pivotal roles played by neutral metal clusters in water decomposition and also opens new avenues toward systematic understanding of water splitting by a large variety of single-cluster catalysts.

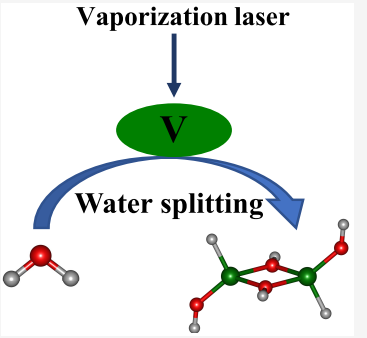

Water splitting is a renewable and environmentally friendly energy source.[1−3] Since surface-supported single atoms/clusters have been demonstrated to boost the catalytic performance in many applications,[4,5] studies of the reactions between water molecules and isolated metal atoms/clusters would help to unravel the microscopic mechanisms of water splitting at the molecular level.[6,7] Pioneering spectroscopic studies of the reactions of water molecules with ionic metals have been carried out, based on the advantages of straightforward detection and size selection.[8−11] The conventional products are the $M^+(H_2O)_n$ solvation complexes, in which the water molecules are weakly bound to the ionic metals.[12] A few insertion complexes of $HMOH^+(H_2O)_n$ are accessible for M = Al, V, Mn.[13−18]

In contrast, experimental investigation of the reactions between the water molecules and neutral metals is significantly more challenging, because the lack of a charge makes size selection of the neutral clusters difficult. The cryogenic matrix-isolation experimental method has afforded valuable spectroscopic information. Studies on the reactions between the water molecules and neutral early transition metal atoms indicated that the HMOH intermediates could undergo either hydrogen production or photochemical isomerization to H_2MO.[19−24] The water molecules react with neutral late-transition metal and lanthanide metal atoms to form the solvation complexes, which can be transformed to the insertion complexes by ultraviolet irradiation.[25−29] The H_2ThO and H_2UO insertion products have also been observed in the cryogenic argon matrices.[30,31]

Recent studies have indicated that the vanadium metals are widely used in the processes of water splitting.[32,33] As the smallest vanadium cluster, neutral vanadium dimer is a model system for providing the structure and energetic information that is difficult to extract from the bulk experiments. Here we report a mass-selected infrared (IR) spectroscopic study of the reactions between the water molecules and neutral vanadium dimer based on threshold photoionization using a vacuum ultraviolet (VUV) laser. The $V_2O_3H_4$ and $V_2O_4H_6$ products are found to have the intriguing $V_2(\mu_2\text{-OH})(\mu_2\text{-H})(\eta^1\text{-OH})_2$ and $V_2(\mu_2\text{-OH})_2(\eta^1\text{-H})_2(\eta^1\text{-OH})_2$ structures, indicating that the water splitting by neutral vanadium dimer proceeds efficiently in the gas phase.

The $V_2O_3H_4$ and $V_2O_4H_6$ target products were generated via laser vaporization in a supersonic expansion of 0.1% H_2O/helium. The IR spectra of $V_2O_3H_4$ and $V_2O_4H_6$ were measured using an IR-VUV spectroscopy apparatus (see the Supporting Information for experimental details).[34,35] A tunable IR optical parametric oscillator/optical parametric amplifier system (LaserVision) was used for IR excitation of $V_2O_3H_4$ and $V_2O_4H_6$, and a VUV light at 193 nm was used for subsequent photoionization with a delay of about 80 ns. The linear

Received: March 7, 2023
Accepted: April 13, 2023

https://doi.org/10.1021/acs.jpclett.3c00637
J. Phys. Chem. Lett. 2023, 14, 3878−3883

relationship of predissociation yield with photon flux was studied by the IR power dependence of the signal.

Figures 1a and 2a show the measured IR spectra of the $V_2O_3H_4$ and $V_2O_4H_6$ products, respectively. Table 1 lists the

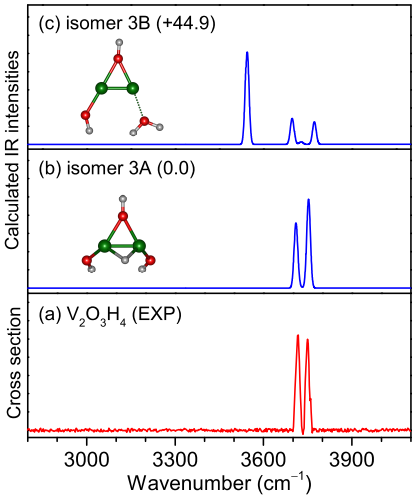

Figure 1. Comparison of experimental IR spectrum (a) of neutral $V_2O_3H_4$ complex and calculated IR spectra (b and c) of the two types of isomers. Calculations were performed at the BPW91/6-311++G(d,p) (O, H)/6-311G (V) level of theory, with the harmonic frequencies scaled by 0.99. The structures of the 3A and 3B isomers are embedded in the inset (O, red; H, light gray; V, olive). Relative energies (in parentheses) are listed in kcal/mol.

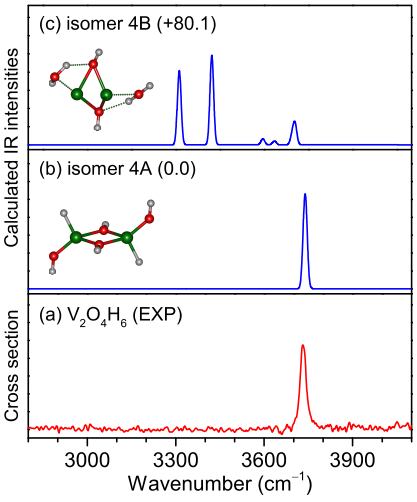

Figure 2. Comparison of experimental IR spectrum (a) of neutral $V_2O_4H_6$ complex and calculated IR spectra (b and c) of the two types of isomers. Calculations were performed at the BPW91/6-311++G(d,p) (O, H)/6-311G (V) level of theory, with the harmonic frequencies scaled by 0.99. The structures of the 4A and 4B isomers are embedded in the inset (O, red; H, light gray; V, olive). Relative energies (in parentheses) are listed in kcal/mol.

corresponding band positions. The experimental spectrum of $V_2O_3H_4$ shows two bands at 3717.5 and 3749.6 cm^{-1} (Figure 1a), and that of $V_2O_4H_6$ consists of a single band at 3732.0 cm^{-1} (Figure 2a). Quantum chemical calculations were carried out at the BPW91/6-311++G(d,p) (O, H)/6-311G (V) level of theory to identify the low-lying structures of the $V_2O_3H_4$ and $V_2O_4H_6$ complexes and to interpret the experimental spectra (see the Supporting Information for theoretical

Table 1. Comparison of the Experimental Band Positions (cm^{-1}) of Neutral $V_2O_3H_4$ and $V_2O_4H_6$ Complexes to the Calculated Values of the Most Stable Structures (Isomers 3A and 4A) Obtained at the BPW91/6-311++G(d,p) (O, H)/6-311G (V) Level of Theory[a]

Species	Exptl	Calcd	Mode
$V_2O_3H_4$	3717.5	3710.7 (60)	symmetric stretching mode of terminal OH groups
		3721.7 (1)	antisymmetric stretching mode of terminal OH groups
	3749.6	3752.9 (82)	stretching mode of bridging OH group
$V_2O_4H_6$	3732.0	3736.6 (191)	antisymmetric stretching mode of bridging OH groups
		3736.7 (1)	symmetric stretching mode of bridging OH groups
		3742.7 (236)	antisymmetric stretching mode of terminal OH groups
		3743.2 (0.1)	symmetric stretching mode of terminal OH groups

[a]IR intensities are listed in parentheses in km/mol, and the calculated harmonic vibrational frequencies are scaled by a factor of 0.99.

details). The optimized structures and calculated IR spectra of $V_2O_3H_4$ and $V_2O_4H_6$ are shown in Figures 1 and 2, respectively. Here, the two types of isomers are named as *n*A and *n*B, respectively, in which *n* denotes the number of oxygen atoms involved in the complex.

For the $V_2O_3H_4$ complex, the most stable isomer has a $V_2(\mu_2{-}OH)(\mu_2\text{-}H)(\eta^1\text{-}OH)_2$ configuration with a ^1A singlet electronic ground state (labeled isomer 3A in Figure 1b), forming an insertion structure. In the second type of isomer (labeled isomer 3B), one water molecule is weakly bound to the V atom, forming a $V_2(\mu_2\text{-}OH)(\eta^1\text{-}OH)(\eta^1\text{-}H_2O)$ solvation structure with a ^1A ground state. Isomer 3B lies higher in energy than isomer 3A by 44.9 kcal/mol, indicating that the water-solvated structure is thermodynamically unstable as compared to the insertion structure. In the simulated IR spectrum of isomer 3A (Figure 1b), the 3710.7 cm^{-1} band is the symmetric stretching mode of terminal OH groups, which is consistent with the experimental band of 3717.5 cm^{-1} (Table 1); the 3752.9 cm^{-1} band is the stretching mode of bridging OH group and agrees with the experimental band of 3749.6 cm^{-1}. However, an intense band at 3544.7 cm^{-1} is predicted in the simulated IR spectrum of isomer 3B (Figure 1c) but is absent in the experimental spectrum, which excludes the existence of isomer 3B.

For the $V_2O_4H_6$ complex, the most stable isomer has a $V_2(\mu_2\text{-}OH)_2(\eta^1\text{-}H)_2(\eta^1\text{-}OH)_2$ structure with a ^1A ground state (labeled isomer 4A in Figure 2b), in which the water molecules are dissociated. Isomer 4B lies 80.1 kcal/mol higher in energy than isomer 4A and consists of a $V_2(\mu_2\text{-}OH)_2(\eta^1\text{-}H_2O)_2$ structure with a ^1A ground state, in which two water molecules are weakly solvated with the V atoms. In the simulated IR spectrum of isomer 4A (Figure 2b), the antisymmetric stretching modes of bridging OH groups and terminal OH groups were calculated to be 3736.6 and 3742.7 cm^{-1} (Table 1), respectively, which are resolved as one band in the experimental spectrum (3732.0 cm^{-1}). The 3312.3 and 3423.2 cm^{-1} bands in the simulated IR spectrum of isomer 4B (Figure 2c) are not detected experimentally. Consequently, the presence of isomer 4B can be ruled out.

The most significant observation in this work is the detection of the water-splitting products rather than the

https://doi.org/10.1021/acs.jpclett.3c00637
J. Phys. Chem. Lett. 2023, 14, 3878−3883

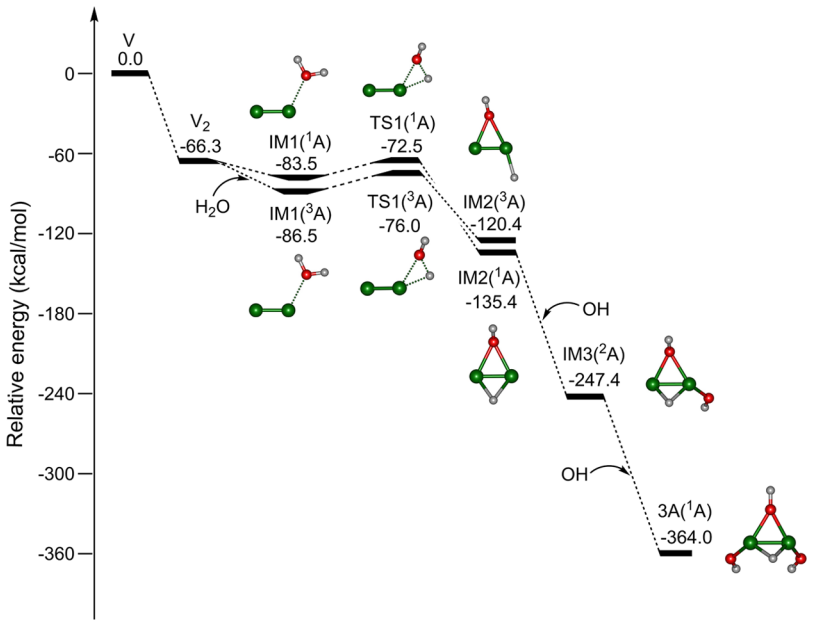

Figure 3. Potential energy profiles for the formation of $V_2O_3H_4$. The abbreviation "IM" stands for intermediate and "TS" for transition state. The corresponding structures are embedded in the inset (O, red; H, light gray; V, olive).

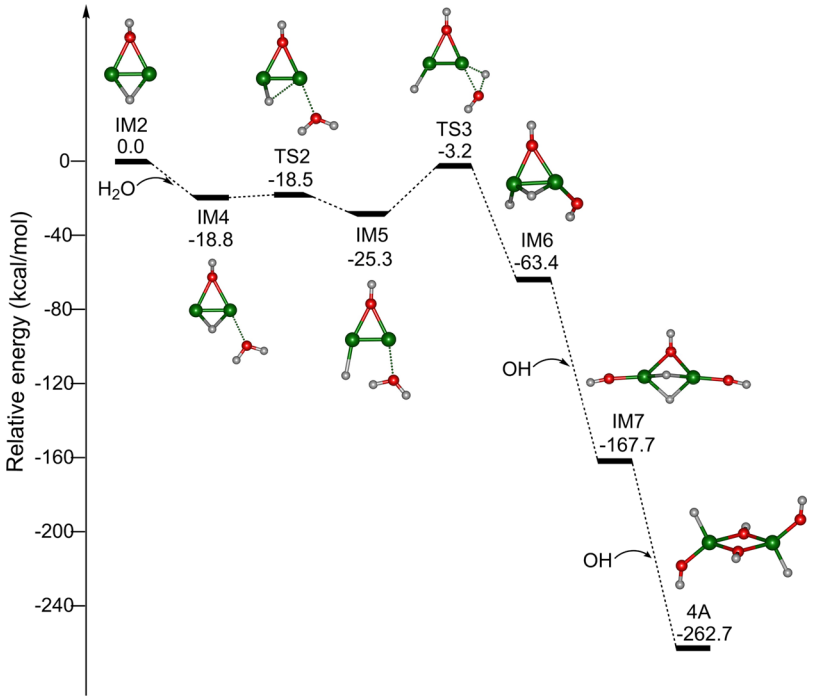

Figure 4. Potential energy profiles for the formation of $V_2O_4H_6$. The abbreviation "IM" stands for intermediate and "TS" for transition state. The corresponding structures are embedded in the inset (O, red; H, light gray; V, olive).

water-solvation complexes. This finding indicates that the water decomposition by V_2 is facile in the gas phase. Since the elementary reactions in the laser-vaporization source are difficult to clarify because of their complexity,[36,37] the possible formation mechanism of the $V_2O_3H_4$ and $V_2O_4H_6$ products were explored by quantum chemical calculations.

The potential energy profiles for the reactions between the water molecules and V_2 were calculated at the BPW91/6-311++G(d,p) (O, H)/6-311G (V) level of theory. While reaction 1 is exothermic by 66.3 kcal/mol,[38] reaction 2 is exothermic by 17.1 kcal/mol. This implies that the dimerization of V atoms is much more favorable than the formation of $V(H_2O)$ from the reaction of V with H_2O. Accordingly, we will mainly focus on the discussion of the pathways for the formation of $V_2O_3H_4$ and $V_2O_4H_6$ beginning from the reactions between V_2 and H_2O.

$$V(^4F) + V(^4F) \rightarrow V_2(^3\Sigma_g^-) \quad (1)$$

$$V(^4F) + H_2O(^1A_1) \rightarrow V(H_2O)(^4A') \quad (2)$$

As shown in Figure 3, the addition of H_2O to V_2 forms the intermediate $IM1(^1A)/IM1(^3A)$, which is predicted to be

https://doi.org/10.1021/acs.jpclett.3c00637
J. Phys. Chem. Lett. 2023, 14, 3878−3883

exothermic by 17.3/20.2 kcal/mol, respectively. The isomerization from IM1(^{1}A) to IM2(^{1}A) is highly exothermic by 51.9 kcal/mol via a transition state (TS1(^{1}A)) with a small barrier of 11.0 kcal/mol. The isomerization from IM1(^{3}A) to IM2(^{3}A) is exothermic by 33.9 kcal/mol via TS1(^{3}A) with a barrier of 10.5 kcal/mol. Considering that IM2(^{1}A) is more stable than IM2(^{3}A) by 15.0 kcal/mol, IM2(^{1}A) is thus considered as a major contributor in the subsequent reactions. This water splitting by V_2 is supported by the absence of water-solvated structures in the present IR-VUV and previous matrix-isolation experiments.[22]

As pointed out previously,[20,21,39] the OH radicals are generated during the laser-vaporization process and might take part in the combination reactions with other species. With this context, the reaction of OH radical with IM2(^{1}A) to form IM3(^{2}A) is predicted to be highly exothermic by 112.0 kcal/mol (Figure 3). The combination of OH and IM3(^{2}A) to produce isomer 3A is also calculated to be extremely exothermic by 116.6 kcal/mol. The above formation mechanisms of $V_2O_3H_4$ are not exclusive. For instance, minor contribution from the combination of H radicals with other fragments is also likely, although the lifetime of the H radical is very short. On the other hand, the formation of $V_2O_3H_4$ may begin with the generation of mononuclear complexes from the reactions between V and H_2O and then proceeds with the aggregation of the relevant mononuclear complexes.

Figure 4 shows the formation profiles of $V_2O_4H_6$. The reaction of IM2 with H_2O to produce IM4 is predicted to be exothermic by 18.8 kcal/mol. The isomerization from IM4 to IM5 is exothermic by 6.5 kcal/mol via a transition state (TS2) with a very small barrier of 0.3 kcal/mol. IM5 could undergo isomerization to generate IM6, which releases 38.1 kcal/mol of energy with a 22.1 kcal/mol barrier (TS3). The reaction of IM6 with the first and second OH radical is calculated to be extremely exothermic by 104.3 and 95.0 kcal/mol, respectively. Consequently, the formation of $V_2O_4H_6$ is both thermodynamically exothermic and kinetically facile in the gas phase, which is consistent with the experimental observations.

In summary, the water molecules reacted with neutral vanadium dimer in the gas phase to form the $V_2O_3H_4$ and $V_2O_4H_6$ products, which were determined to have the $V_2(\mu_2\text{-OH})(\mu_2\text{-H})(\eta^1\text{-OH})_2$ and $V_2(\mu_2\text{-OH})_2(\eta^1\text{-H})_2(\eta^1\text{-OH})_2$ structures. The water decomposition by V_2 was found to occur readily in the present experimental conditions. The formation of $V_2O_3H_4$ and $V_2O_4H_6$ from the reaction between water and V_2 was theoretically predicted to be both thermodynamically exothermic and kinetically facile in the gas phase, which supports the experimentally observed features. These findings may stimulate further systematic studies of the reactions of water molecules with a large variety of neutral main-group and transition metal clusters.

■ ASSOCIATED CONTENT

Supporting Information

The Supporting Information is available free of charge at https://pubs.acs.org/doi/10.1021/acs.jpclett.3c00637.

Additional experimental details and theoretical methods; mass spectra of the products (Figure S1); comparison of experimental and calculated IR spectra of $V_2O_3H_4$ (Figure S2); comparison of experimental and calculated IR spectra of $V_2O_4H_6$ (Figure S3); Cartesian coordinates of the low-lying isomers, intermediates, and transition states; supporting references (PDF)

Transparent Peer Review report available (PDF)

■ AUTHOR INFORMATION

Corresponding Authors

Gang Li − *State Key Laboratory of Molecular Reaction Dynamics, Dalian Institute of Chemical Physics, Chinese Academy of Sciences, Dalian 116023, China;* orcid.org/0000-0001-5984-111X; Email: gli@dicp.ac.cn

Ling Jiang − *State Key Laboratory of Molecular Reaction Dynamics, Dalian Institute of Chemical Physics, Chinese Academy of Sciences, Dalian 116023, China; Hefei National Laboratory, Hefei 230088, China;* orcid.org/0000-0002-8485-8893; Email: ljiang@dicp.ac.cn

Authors

Huijun Zheng − *State Key Laboratory of Molecular Reaction Dynamics, Dalian Institute of Chemical Physics, Chinese Academy of Sciences, Dalian 116023, China; University of Chinese Academy of Sciences, Beijing 100049, China;* orcid.org/0000-0003-2876-7580

Shuai Jiang − *State Key Laboratory of Molecular Reaction Dynamics, Dalian Institute of Chemical Physics, Chinese Academy of Sciences, Dalian 116023, China*

Wenhui Yan − *State Key Laboratory of Molecular Reaction Dynamics, Dalian Institute of Chemical Physics, Chinese Academy of Sciences, Dalian 116023, China; University of Chinese Academy of Sciences, Beijing 100049, China*

Tiantong Wang − *State Key Laboratory of Molecular Reaction Dynamics, Dalian Institute of Chemical Physics, Chinese Academy of Sciences, Dalian 116023, China; University of Chinese Academy of Sciences, Beijing 100049, China*

Shangdong Li − *State Key Laboratory of Molecular Reaction Dynamics, Dalian Institute of Chemical Physics, Chinese Academy of Sciences, Dalian 116023, China; University of Chinese Academy of Sciences, Beijing 100049, China*

Hua Xie − *State Key Laboratory of Molecular Reaction Dynamics, Dalian Institute of Chemical Physics, Chinese Academy of Sciences, Dalian 116023, China;* orcid.org/0000-0003-2091-6457

Xueming Yang − *State Key Laboratory of Molecular Reaction Dynamics, Dalian Institute of Chemical Physics, Chinese Academy of Sciences, Dalian 116023, China; Hefei National Laboratory, Hefei 230088, China; Department of Chemistry and Shenzhen Key Laboratory of Energy Chemistry, Southern University of Science and Technology, Shenzhen 518055, China;* orcid.org/0000-0001-6684-9187

Complete contact information is available at: https://pubs.acs.org/10.1021/acs.jpclett.3c00637

Notes

The authors declare no competing financial interest.

■ ACKNOWLEDGMENTS

The authors gratefully acknowledge the Dalian Coherent Light Source (DCLS) for support and assistance. This work was supported by the National Key Research and Development Program of China (2021YFA1400501), the National Natural Science Foundation of China (Grant Nos. 22125303, 92061203, 92061114, 21327901, 21976049, 22103082, 22273101, and 22288201), the Youth Innovation Promotion

Association of the Chinese Academy of Sciences (CAS) (2020187), Innovation Program for Quantum Science and Technology (2021ZD0303304), CAS (GJJSTD20220001), Dalian Institute of Chemical Physics (DICP DCLS201702), International Partnership Program of CAS (121421KYSB20170012), and K. C. Wong Education Foundation (GJTD-2018-06).

REFERENCES

(1) Fujishima, A.; Honda, K. Electrochemical Photolysis of Water at a Semiconductor Electrode. *Nature* **1972**, *238*, 37−38.
(2) Takata, T.; Jiang, J.; Sakata, Y.; Nakabayashi, M.; Shibata, N.; Nandal, V.; Seki, K.; Hisatomi, T.; Domen, K. Photocatalytic Water Splitting with a Quantum Efficiency of Almost Unity. *Nature* **2020**, *581*, 411−414.
(3) Li, X.-P.; Huang, C.; Han, W.-K.; Ouyang, T.; Liu, Z.-Q. Transition Metal-based Electrocatalysts for Overall Water Splitting. *Chin. Chem. Lett.* **2021**, *32*, 2597−2616.
(4) Li, J.; Li, Y.; Zhang, T. Recent Progresses in the Research of Single-Atom Catalysts. *Sci. China: Mater.* **2020**, *63*, 889−891.
(5) Sun, L.; Reddu, V.; Wang, X. Multi-Atom Cluster Catalysts for Efficient Electrocatalysis. *Chem. Soc. Rev.* **2022**, *51*, 8923−8956.
(6) Heiz, U.; Bullock, E. L. Fundamental Aspects of Catalysis on Supported Metal Clusters. *J. Mater. Chem.* **2004**, *14*, 564−577.
(7) Chakraborty, I.; Pradeep, T. Atomically Precise Clusters of Noble Metals: Emerging Link between Atoms and Nanoparticles. *Chem. Rev.* **2017**, *117*, 8208−8271.
(8) Irigoras, A.; Fowler, J. E.; Ugalde, J. M. Reactivity of $Sc^+(^3D, ^1D)$ and $V^+(^5D, ^3F)$: Reaction of Sc^+ and V^+ with Water. *J. Am. Chem. Soc.* **1999**, *121*, 574−580.
(9) Vaden, T. D.; Weinheimer, C. J.; Lisy, J. M. Evaporatively Cooled $M^+(H_2O)Ar$ Cluster Ions: Infrared Spectroscopy and Internal Energy Simulations. *J. Chem. Phys.* **2004**, *121*, 3102−3107.
(10) Walters, R. S.; Pillai, E. D.; Duncan, M. A. Solvation Dynamics in $Ni^+(H_2O)_n$ Clusters Probed with Infrared Spectroscopy. *J. Am. Chem. Soc.* **2005**, *127*, 16599−16610.
(11) Reveles, J. U.; Calaminici, P.; Beltran, M. R.; Koster, A. M.; Khanna, S. N. H_2O Nucleation around Au^+. *J. Am. Chem. Soc.* **2007**, *129*, 15565−15571.
(12) Walker, N. R.; Walters, R. S.; Duncan, M. A. Frontiers in the Infrared Spectroscopy of Gas Phase Metal Ion Complexes. *New J. Chem.* **2005**, *29*, 1495−1503.
(13) Heller, J.; Tang, W. K.; Cunningham, E. M.; Demissie, E. G.; vav der Linde, C.; Lam, W. K.; Oncak, M.; Siu, C.-K.; Beyer, M. K. Getting Ready for the Hydrogen Evolution Reaction: The Infrared Spectrum of Hydrated Aluminum Hydride-Hydroxide $HAl-OH^+(H_2O)_{n-1}$ (n = 9−14). *Angew. Chem., Int. Ed.* **2021**, *60*, 16858−16863.
(14) Heller, J.; Pascher, T. F.; Muss, D.; van der Linde, C.; Beyer, M. K.; Oncak, M. Photochemistry and UV/vis Spectroscopy of Hydrated Vanadium Cations, $V^+(H_2O)_n$ (n = 1−41), A Model System for Photochemical Hydrogen Evolution. *Phys. Chem. Chem. Phys.* **2021**, *23*, 22251−22262.
(15) Heller, J.; Pascher, T. F.; van der Linde, C.; Oncak, M.; Beyer, M. K. Photochemical Hydrogen Evolution at Metal Centers Probed with Hydrated Aluminium Cations, $Al^+(H_2O)_n$, n = 1−10. *Chem. Eur. J.* **2021**, *27*, 16367−16376.
(16) Heller, J.; Cunningham, E. M.; Hartmann, J. C.; van der Linde, C.; Oncak, M.; Beyer, M. K. Size-Dependent H and H_2 Formation by Infrared Multiple Photon Dissociation Spectroscopy of Hydrated Vanadium Cations, $V^+(H_2O)_n$, n = 3−51. *Phys. Chem. Chem. Phys.* **2022**, *24*, 14699−14708.
(17) Heller, J.; Cunningham, E. M.; van der Linde, C.; Oncak, M.; Beyer, M. K. Infrared Multiple Photon Dissociation Spectroscopy Confirms Reversible Water Activation in $Mn^+(H_2O)_n$, $n \leq 8$. *J. Phys. Chem. Lett.* **2022**, *13*, 3269−3275.
(18) Xin, K.; Chen, Y.; Zhang, L.; Xu, B.; Wang, X.; Wang, G. Infrared Photodissociation Spectroscopic Investigation on VO^+ and NbO^+ Hydrolysis Catalyzed by Water Molecules. *Phys. Chem. Chem. Phys.* **2021**, *23*, 528−535.
(19) Kauffman, J. W.; Hauge, R. H.; Margrave, J. L. Reactions of Atomic Scandium, Titanium, and Vanadium with Molecular Water at 15 K. *J. Phys. Chem.* **1985**, *89*, 3547−3552.
(20) Zhang, L. N.; Dong, J.; Zhou, M. F. Matrix-Isolation Fourier Transform Infrared and Theoretical Studies of Laser-Ablated Sc Atom Reactions with Water Molecules. *J. Phys. Chem. A* **2000**, *104*, 8882−8886.
(21) Zhang, L. N.; Shao, L. M.; Zhou, M. F. Reactions of Laser-Ablated Y and La Atoms with H_2O Infrared Spectra and Density Functional Calculations of the HMO, HMOH and $M(OH)_2$ Molecules in Solid Argon. *Chem. Phys.* **2001**, *272*, 27−36.
(22) Zhou, M. F.; Zhang, L. N.; Dong, J.; Qin, Q. Z. Reactions of Group IV Metal Atoms with Water Molecules. Matrix Isolation FTIR and Theoretical Studies. *J. Am. Chem. Soc.* **2000**, *122*, 10680−10688.
(23) Zhou, M. F.; Dong, J.; Zhang, L. N.; Qin, Q. Z. Reactions of Group V Metal Atoms with Water Molecules. Matrix Isolation FTIR and Quantum Chemical Studies. *J. Am. Chem. Soc.* **2001**, *123*, 135−141.
(24) Macrae, V. A.; Downs, A. J. Matrix Studies of the Thermal and Photolytic Reactions of Ga Vapour Species with H_2O: Formation and Characterisation of the Adducts $Ga-OH_2$ and Ga_2-OH_2 and the Photoproducts HGaOH, GaOH and Ga(mu-H)(mu-OH)Ga. *Phys. Chem. Chem. Phys.* **2004**, *6*, 4571−4578.
(25) Kauffman, J. W.; Hauge, R. H.; Margrave, J. L. Studies of Reactions of Atomic and Dlatomlc Cr, Mn, Fe, Co, Ni, Cu, and Zn with Molecular Water at 15 K. *J. Phys. Chem.* **1985**, *89*, 3541−3547.
(26) Zhou, M. F.; Zhang, L. N.; Shao, L. M.; Wang, W. N.; Fan, K. N.; Qin, Q. Z. Reactions of Mn with H_2O and MnO with H_2. Matrix-Isolation FTIR and Quantum Chemical Studies. *J. Phys. Chem. A* **2001**, *105*, 5801−5807.
(27) Zhang, L. N.; Zhou, M. F.; Shao, L. M.; Wang, W. N.; Fan, K. N.; Qin, Q. Z. Reactions of Fe with H_2O and FeO with H_2. A Combined Matrix Isolation FTIR and Theoretical Study. *J. Phys. Chem. A* **2001**, *105*, 6998−7003.
(28) Xu, J.; Zhou, M. Reactions of Early Lanthanide Metal Atoms (Nd, Sm, Eu) with Water Molecules. A Matrix Isolation Infrared Spectroscopic and Theoretical Study. *J. Phys. Chem. A* **2006**, *110*, 10575−10582.
(29) Xu, J.; Jin, X.; Zhou, M. Reactions of Late Lanthanide Metal Atoms with Water Molecules: A Matrix Isolation Infrared Spectroscopic and Theoretical Study. *J. Phys. Chem. A* **2007**, *111*, 7105−7111.
(30) Liang, B. Y.; Andrews, L.; Li, J.; Bursten, B. E. Experimental and Theoretical Studies of the Products of Laser-Ablated Thorium Atom Reactions with H_2O in Excess Argon. *J. Am. Chem. Soc.* **2002**, *124*, 6723−6733.
(31) Liang, B.; Hunt, R. D.; Kushto, G. P.; Andrews, L.; Li, J.; Bursten, B. E. Reactions of Laser-Ablated Uranium Atoms with H_2O in Excess Argon: A Matrix Infrared and Relativistic DFT Investigation of Uranium Oxyhydrides. *Inorg. Chem.* **2005**, *44*, 2159−2168.
(32) Kim, T. W.; Choi, K.-S. Nanoporous $BiVO_4$ Photoanodes with Dual-Layer Oxygen Evolution Catalysts for Solar Water Splitting. *Science* **2014**, *343*, 990−994.
(33) Wang, L.; Shi, X.; Jia, Y.; Cheng, H.; Wang, L.; Wang, Q. Recent Advances in Bismuth Vanadate-based Photocatalysts for Photoelectrochemical Water Splitting. *Chin. Chem. Lett.* **2021**, *32*, 1869−1878.
(34) Zhang, B.; et al. Infrared Spectroscopy of Neutral Water Dimer Based on a Tunable Vacuum Ultraviolet Free Electron Laser. *J. Phys. Chem. Lett.* **2020**, *11*, 851−855.
(35) Li, G.; Wang, C.; Zheng, H.-J.; Wang, T.-T.; Xie, H.; Yang, X.-M.; Jiang, L. Infrared Spectroscopy of Neutral Clusters Based on a Vacuum Ultraviolet Free Electron Laser. *Chin. J. Chem. Phys.* **2021**, *34*, 51−60.
(36) Zhou, M. F.; Andrews, L.; Bauschlicher, C. W. Spectroscopic and Theoretical Investigations of Vibrational Frequencies in Binary

https://doi.org/10.1021/acs.jpclett.3c00637
J. Phys. Chem. Lett. 2023, 14, 3878−3883

Unsaturated Transition-Metal Carbonyl Cations, Neutrals, and Anions. *Chem. Rev.* **2001**, *101*, 1931−1961.
(37) Duncan, M. A. Laser Vaporization Cluster Sources. *Rev. Sci. Instrum.* **2012**, *83*, No. 041101.
(38) Wu, X. Y.; Ray, A. K. A Density Functional Study of Small Neutral and Cationic Vanadium Clusters V_n and V_n^+ (n = 2−9). *J. Chem. Phys.* **1999**, *110*, 2437−2445.
(39) Suzer, S.; Andrews, L. Matrix Isolation Study of Electron Impact on H_2O. Infrared Spectrum of OH^- in Solid Argon. *J. Chem. Phys.* **1988**, *88*, 916−921.

https://doi.org/10.1021/acs.jpclett.3c00637
J. Phys. Chem. Lett. 2023, 14, 3878−3883